nature microbiology

Article

https://doi.org/10.1038/s41564-023-01593-7

Ammonia-oxidizing bacteria and archaea exhibit differential nitrogen source preferences

In the format provided by the authors and unedited

Supplementary Discussion

Stable isotope tracing of the cellular fate of N in *N. oceani* and *N. inopinata*

The ^{15}N-labelling approach was used to track the fate of N species in the growth experiments of *N. oceani* and *N. inopinata* (Extended Data Figs. 3c–f, 9, Supplementary Fig. 7). As indicated by the unlabeled growth experiments (Fig. 1g), the simultaneous consumption of ammonia and urea by the γ-AOB *N. oceani* was examined using the same ^{15}N-labeling approach as described for *N. lacus* labeling experiments (Fig. 2). Cultures inoculated with ammonia-preadapted *N. oceani* cells immediately converted $^{15}NH_3$ to $^{15}NO_2^-$ during the lag phase (0–100 h) (Extended Data Fig. 9a). In the parallel experiment, very little $^{15}NO_2^-$ derived from ^{15}N-urea during lag phase (Extended Data Fig. 9c). The percentage of $^{15}NO_2^-$ originating from ^{15}N-urea then gradually increased from ~3% to ~60% during exponential growth (Extended Data Fig. 9c), which was coupled with a continuous decrease in the contribution from NH_3, a shown in the parallel experiment tracing $^{15}NH_3$ to $^{15}NO_2^-$ production throughout the remaining growth period (Extended Data Fig. 9a). Although no net accumulation of ammonia was observed in unlabeled growth experiments, a substantial amount of $^{15}NH_3$ (~55%) was released into the medium during ^{15}N-urea hydrolysis (Extended Data Fig. 3d, Supplementary Fig. 7). The release of $^{15}NH_3$ was closely correlated with $^{15}NO_2^-$ production ($R^2 = 0.99$, $P < 0.01$) in the ^{15}N-urea labeling experiments (Supplementary Fig. 7). Thus, about 45% of the ammonia released to the medium during urea hydrolysis was rapidly oxidized to nitrite.

Unlike the AOA species, comammox *N. inopinata* showed a weaker repression of urea utilization and started to use urea before ammonia was fully exhausted (Fig. 1c). In incubations with added ^{15}N-urea, the urea-derived ^{15}N atoms appeared in the extracellular pools of nitrite, nitrate, and ammonia ~75 h after incubation, showing that *N. inopinata* turned on urea utilization significantly prior to ammonia depletion (at ~100 h) and suggesting a mechanism for anticipatory transition to urea consumption (Extended Data Fig. 3f). This transition was

associated with a reduction in growth rate when consuming ammonia in the mixed N species medium compared to growth in the ammonia-only medium ($P < 0.001$) (Fig. 1c), presumably because of the metabolic burden of expressing urea utilization genes while ammonia was still present. After the complete shift to urea consumption (~100 h), the secreted $^{15}NH_3$ decreased to below the level of detection (1 nM) (Extended Data Fig. 3f).

Preferred nitrogen substrate assimilation in AOA, comammox, and γ-AOB species

Similar to β-AOB *N. lacus*, we conducted a parallel set of labeling experiments with marine AOA *N. piranensis*, soil AOA *N. viennensis*, and comammox *N. inopinata* (Extended Data Fig. 4a), and examined their ammonia- and urea-N assimilation at single-cell resolution using NanoSIMS. In contrast to *N. lacus,* they all preferentially assimilated N from ammonia at T1 with 99.3 ± 3.5%, 95.2 ± 3.3%, and 90.7 ± 7.9% new N incorporation from ammonia and 0.7 ± 0.0%, 4.8 ± 0.2%, and 9.3 ± 0.7% from urea for *N. piranensis*, *N. viennensis*, and *N. inopinata*, respectively (Extended Data Fig. 4b, c). At T2, new N incorporation from urea and ammonia was roughly equivalent at 43.5–56.5% (Extended Data Fig. 4b, c). For the third type of behavior shown by the γ-AOB *N. oceani*, we found similar new N incorporation from urea and ammonia in late exponential phase (49.0–51.0%) (Extended Data Fig. 4b, c), showing that γ-AOB co-assimilated ammonia and urea.

Distinct responses of AOA and comammox species after transitioning to consumption of the secondary N substrate

Although the characterized AOA and comammox species all prefer ammonia as their primary energy and N source, there was large variation in their adaptive transition from ammonia to urea metabolism. The marine AOA *N. piranensis* demonstrated a pronounced reduction in growth rate upon ammonia depletion, while the soil AOA *N. viennensis* showed negligible lag when grown on a mixture of ammonia and urea (Fig. 1a, b). The comammox species *N. inopinata* initiated urea utilization ~25 hours before ammonia exhaustion (Extended Data Fig. 3f), possibly

reflecting an adaptive mechanism to use the alternative substrate before ammonia depletion but at the cost of the added biosynthetic burden slowing growth before full transition (Fig. 1c). In contrast, both characterized marine and soil AOA species repressed use of urea, growing on ammonia at comparable rates in the presence or absence of urea before transitioning to urea consumption (Fig. 1a, b).

In addition, we characterized the response of AOA and comammox species to the switch from a single N substrate to ammonia-urea mixture. The addition of urea to the AOA *N. piranensis* and *N. viennensis* did not interrupt their growth on ammonia. Both organisms repressed the consumption of urea until ammonia was depleted (Fig. 4a, b). However, they differed in the growth kinetics of substrate transition. *N. viennensis* sustained active growth during transition whereas *N. piranensis* exhibited a significant lag (Fig. 4a, b). With the alternate order of addition, growth of both species slowed upon ammonia addition and active ammonia consumption was delayed until near depletion of urea. (Fig. 4a, b). Unlike the AOA species, the comammox *N. inopinata* showed much weaker repression of urea consumption in the presence of ammonia and immediately consumed urea upon its addition to ammonia-growing cultures (Fig. 4c).

We also characterized the oxygen uptake activity of AOA and comammox species after addition of low concentrations of ammonia and urea using microrespirometry (Extended Data Fig. 10). Following multiple subculturing in ammonia or urea-only media, we observed instantaneous oxygen consumption upon addition of low concentrations of ammonia (20–40 μM) or urea (10–20 μM) to urea-grown *N. piranensis* and *N. viennensis* cells at early stationary phase (Extended Data Fig. 10d, e). No discernible stimulation of O_2 uptake was observed for multiple hours when 10 μM urea was added to ammonia-grown cells immediately following their depletion of ammonia from the medium (Extended Data Fig. 10a, b). This further indicated that these AOA species repress urea utilization while growing on ammonia and that a significant period of adaptation is required before their transition to growth on urea. Repression of growth on urea is

also consistent with AOA having evolved as specialists in competition for ammonia in mixed-nutrient environments (Figs. 3 and 4). In contrast, both ammonia- and urea-adapted comammox *N. inopinata* responded quickly to addition of either substrate (Extended Data Fig. 10c, f). Thus, comammox appeared to function as a generalist, having relatively high affinity for both substrates but less stringent regulation. Previous studies have demonstrated a remarkable metabolic versatility among *Nitrospira* species [1]. Thus, it would also be of interest to investigate whether *N. inopinata* utilizes other organic N sources and if it possesses high affinity transporters for these substrates as well. Such unique adaptive features could provide *N. inopinata*-like comammox species with a competitive advantage in environments with variable supplies of inorganic and organic N substrates [2].

P_{II} proteins and their modifying enzymes control the selective N source uptake regulation in AOM

Our combined analyses clearly implicated GlnB-type P_{II} proteins in controlling the uptake of extracellular N species through interaction with AMT. This family of proteins have well characterized functions in modulating the uptake of ammonia used for assimilation [34,35] but little is known about how they function in organisms that use ammonia for both anabolic synthesis and catabolic energy generation. In well characterized heterotrophs, the transport of ammonia by the AMT can be blocked by binding to the GlnB protein. Binding to GlnB is controlled by its post-translational modification by a second regulatory protein (GlnD) in response to variations in intracellular glutamine and 2-oxoglutarate levels [3-7]. Although GlnB-type P_{II} proteins are common in all major lineages of AOM, they are not always associated with GlnD. A homolog of GlnD could not be identified in AOA and is variably distributed among AOB (Extended Data Fig. 1a, b). It is present in *Nitrosospira* β-AOB and *Nitrosococcus* γ-AOB but absent in *Nitrosomonas* β-AOB (Extended Data Fig. 1b).

101 *N. lacus* carries the full canonical set of N uptake regulatory genes. The absence of any apparent
102 lag in the growth of *N. lacus* with depletion of urea in the mixed N medium, and blocked
103 transport of ammonia before urea depletion, were consistent with GlnB-type P_{II} protein control
104 of ammonia uptake (Figs. 1d and 2). Since this P_{II} protein is the only known substrate for GlnD
105 [7], and *glnD* was transcribed at significantly higher levels ($P = 6.57 \times 10^{-15}$) during ammonia
106 uptake repression (Fig. 4d), our data strongly suggest GlnB-type P_{II} protein was post-
107 translationally modified by GlnD via reversible uridylylation and deuridylylation. Although the
108 activity of GlnD is known to be controlled by intracellular glutamine levels as a measure of
109 cellular N sufficiency [6,7], the absence of any change in growth rate with transition from urea to
110 growth on ammonia suggested that ammonia was never limiting. Nitrogen sufficiency
111 throughout growth was also indicated by relatively unaltered transcription of genes coding for
112 ammonia assimilation enzymes, such as glutamate dehydrogenase (GDH), glutamine synthetase
113 (GS), and the GS modifying enzyme glutamine synthetase adenylyltransferase (GlnE)
114 (Supplementary Table 3). Assuming that levels of glutamine and other known intracellular
115 metabolites did not signal N deficiency, GlnD might be responding to the availability of an
116 effector molecule other than glutamine, possibly urea, in *Nitrosospira* β-AOB species.

117 Unlike *N. lacus*, the AOA species repressed urea uptake and utilization when cells were using
118 ammonia and demonstrated a more complex role of P_{II} proteins. The *N. piranensis* genome
119 harbors two copies of DUR3-type urea transporters (NPIRD3C_1395 and NPIRD3C_1384), and
120 only NPIRD3C_1395 was highly transcribed on urea, suggesting it was mainly responsible for
121 urea uptake. *N. piranensis* also encodes two ammonia transporter genes, *amt1* and *amt2*,
122 suggested to have high and low affinity for ammonia, respectively, based on their similarity to
123 transporters characterized in *Nitrosopumilus maritimus* [8-10]. The *amt1* gene was constitutively
124 transcribed under all growth conditions (Fig. 4a). Transcription of the lower affinity *amt2*
125 (NPIRD3C_1670), transcribed at much lower levels than *amt1* (Fig. 4a), was elevated in the
126 presence of ammonia (AU-T1 and T2) and in response to ammonia addition to cultures growing

127 on urea (UA-T2 vs. T1), and depressed upon ammonia depletion (AU-T3 and T4). The
128 differential response of *amt2* relative to *amt1* suggests *amt2* may have additional functions other
129 than ammonia uptake.

130 Two *glnB*-like genes (*glnB1* and *glnB2*, NPIRD3C_1671 and NPIRD3C_1673) flank the
131 downstream region of *amt2* (Extended Data Fig. 2). Intriguingly, *glnB1* (NPIRD3C_1671) was
132 significantly downregulated ($P = 3.5 \times 10^{-20}$) and the high affinity *amt1* significantly upregulated
133 after switching from ammonia to urea consumption and vice versa upon ammonia introduction
134 into urea-grown cells (Fig. 4a). The second *glnB*-like gene (NPIRD3C_2171) showed the
135 opposite transcription pattern (Fig. 4a). Although constitutively transcribed at relatively high
136 levels in *N. piranensis*, it was significantly upregulated ($P = 9.3 \times 10^{-4}$) with transition from
137 ammonia to urea (AU-T3 vs. T2) and significantly repressed ($P = 2.7 \times 10^{-56}$) in response to the
138 addition of ammonia (UA-T2 vs. T1). These results strongly suggest a role for these P_{II} proteins
139 in coordinating the activities of *amt1* and *amt2* in ammonia transport and the sensing of cellular
140 N status.

141 Differential transcription of two putative *glnB* genes was also observed in the soil AOA *N.*
142 *viennensis* (NVIE_013340, NVIE_014550) in response to ammonia and urea additions. Their
143 transcription levels were significantly higher ($P < 0.01$) following urea spike and were
144 significantly lower ($P < 0.01$) after ammonia introduction (Fig. 4b).

145 Two *glnB* genes (NPIRD3C_1671 and NPIRD3C_2171) in marine AOA *N. piranensis* showed
146 opposite patterns of elevated transcription in response to extracellular ammonia and urea
147 availabilities (Fig. 4a), suggesting they may carry out potentially complementary regulatory
148 functions to cooperatively control influx of ammonia and urea in marine AOA. A range of
149 different transporters have been recently identified as new P_{II} protein targets, including urea
150 transporters [11]. Thus, it is tempting to speculate that GlnB in AOA can also interact with urea
151 transporters to block the uptake of external urea in the presence of ammonia. Neither *glnB* nor

152 *glnD* gene was differentially transcribed in γ-AOB *N. oceani* (Fig. 4e), which is consistent with
153 the lack of N source repression for this species when grown in a mixture of ammonia and urea.
154 No homolog of *glnB* or *glnD* was identified in most *Nitrosomonas* β-AOB species genomes
155 (Extended Data Fig. 1b), and *Nitrosomonas ureae* lacks the gene encoding GlnD, which may in
156 part explain the weaker repression of ammonia utilization by *Nitrosomonas ureae* compared to
157 *Nitrosospira* species (Fig. 1f).

158 **Transcriptional changes and transcription control of urea hydrolysis pathway genes in *N.***
159 ***lacus***

160 Urea hydrolysis genes (EBAPG3_007765–EBAPG3_007795) were constitutively transcribed in
161 *N. lacus* across all growth phases. Transcripts of the *ureC* gene (EBAPG3_007780) were among
162 the ten-most abundant in the transcriptome of *N. lacus* before urea exhaustion (Supplementary
163 Tables 3 and Source Data Table 1). Although significantly downregulated upon urea depletion
164 ($P = 2.8 \times 10^{-17}$) (A+U T3 vs. T2), transcript abundance remained elevated after switching to
165 using ammonia (Fig. 4d).

166 Regulation of the urease operon is almost certainly controlled by a nickel-responsive regulator
167 (NikR, EBAPG3_007745) located immediately upstream of the urea utilization operon in *N.*
168 *lacus* (Extended Data Fig. 2), which has been shown to control transcription of the *Helicobacter*
169 *pylori* urease [12]. Its transcript abundance decreased ($P = 1.7 \times 10^{-239}$) more than 46-fold upon
170 urea depletion (A+U-T3 vs. T2) (Supplementary Table 3).

171 *N. lacus* encodes enzymes implicated in ATP-dependent urea hydrolysis in other β-AOB species,
172 urea carboxylase and allophanate hydrolase (Extended Data Figs. 1b and 2). However, their low
173 transcription relative to the urease genes during urea consumption by *N. lacus* suggests different
174 functions for these conserved enzymes in β-AOB (Supplementary Table 3).

175 **Limited assimilation of urea-derived C by the tested AOM species**

176 The direct assimilation of urea-derived C by AOM at the single-cell level was confirmed via
177 NanoSIMS analysis, and we compared these incorporation rates to autotrophic C fixation rates
178 (Extended Data Fig. 7). Archaeal and bacterial ammonia oxidizers were grown in ammonia-urea
179 media with either dual-labeled $^{13}C^{15}N$-urea (and unlabeled NH_3 and bicarbonate) or ^{15}N-NH_3 and
180 ^{13}C-bicarbonate (and unlabeled urea). The marine AOA *N. piranensis* incorporated 15.3–21.3%
181 of its total cellular C from bicarbonate but barely incorporated C from urea (0.1–0.3%) across
182 different growth phases (Extended Data Fig. 7a). For the soil AOA *N. viennensis* and the
183 comammox *N. inopinata*, hardly any incorporation of urea-C (~0.1%) was observed when grown
184 on ammonia (T1), and C incorporation from urea increased to 0.5–1.1% after urea depletion (T2)
185 (Extended Data Fig. 7b, c). Consistently, at T2, C incorporation from bicarbonate decreased
186 from 13 ± 4.5% and 5.9 ± 2.0% to 8.0 ± 3.5% and 4.9 ± 1.8% for *N. viennensis* and *N. inopinata*,
187 respectively (Extended Data Fig. 7b, c). The β-AOB *N. lacus*, which preferentially used urea-N
188 over ammonia, incorporated 1.6 ± 0.6% C from urea at T1 (Extended Data Fig. 7d), which was
189 less than from bicarbonate (10.5 ± 0.9% C). The C incorporation from urea decreased to 0.7 ±
190 0.3% at T2 (Extended Data Fig. 7d). The percentage of urea-C incorporation remained relatively
191 unchanged for the γ-AOB *N. oceani* across different growth phases (4.1–4.8%) (Extended Data
192 Fig. 7e). Taken together, although some characterized AOM species were able to use urea-
193 derived C to supplement their C requirement in the presence of bicarbonate and CO_2, they
194 mainly assimilated urea-derived N when grown on urea (Extended Data Figs. 4–7) and urea was
195 not a significant source of cellular carbon.

196 **Potential factors influencing kinetic analysis of AOM species**

197 We do notice some differences among the kinetic data for ammonia oxidation particularly in *N.*
198 *viennensis* between our study and a previous report [13]. Although we can only speculate about the
199 reasons, strains with high specific affinities have been found sensitive to variations in
200 temperature, laboratory handling, and substrate depletion [14]. The higher specific affinities for
201 ammonia of *N. viennensis* (Fig. 3b and Supplementary Table 2) reported here may reflect a more

202 realistic estimate of the maximum specific affinities attainable by this species. Short-term
203 kinetics experiments on whole cells can furthermore be prone to accumulation of intermediates
204 and result in varying respiratory activities [14]. To avoid such metabolic imbalances as much as
205 possible, we grew all cultures at sufficient O_2 to avoid O_2 limitation in late exponential phase and
206 associated possible changes in expression of respiratory complexes. Kinetic properties of all
207 strains were investigated without harvesting of cell material. Only in strains where near steady-
208 state metabolic rates with 20 μM ammonia addition were too low and $K_{m(app)}$ above the range
209 measurable in individual incubations, measurements were conducted by multiple discrete
210 substrate additions with increasing concentrations.

211 **Function of Rhesus-type ammonia transporter in AOM species**

212 Our study indicates that both ammonia assimilation and oxidation are transport-dependent.
213 Although the *rh50 amt* knockout mutant of *Nitrosmonas europaea* can still oxidize ammonia
214 when supplemented with high ammonia concentrations (≥ 1 mM) [15], it is possible that ammonia
215 (NH_3) diffusion alone was likely sufficient to support ammonia oxidation and assimilation for
216 growth in the mutants under conditions of the relatively high ammonia concentrations tested.
217 Indeed, previous studies of ammonia assimilation by *E. coli* have revealed that active ammonia
218 transport via its ammonia transporter was essential for growth when ammonia concentrations
219 were below ~20 μM [16]. At higher ammonia concentrations, passive membrane diffusion
220 becomes a major source of ammonia for biosynthesis in *E. coli* [16]. Considering that ~99% of the
221 consumed ammonia was oxidized, while only ~1% was assimilated by *N. europaea*, it has been
222 proposed that ammonia uptake capacity is regulated based on the demands of energy generation,
223 rather than N assimilation [17].

224 Both AOB and clade A comammox species encode Rh50-type AMTs, however, their
225 characterized species have shown distinct affinities for ammonia [13]. While the Rh50-type AMT
226 of *N. europaea* has been previously characterized as a low-affinity AMT [18], recent studies have

227 indicated that even minor alterations to a twin histidine motif of AMTs can increase their affinity
228 for ammonium by more than 10-fold [19]. Also, given that ammonia transport is essential for
229 anabolism, the presence of a low-affinity AMT in *N. inopinata* appears incompatible with its
230 oligotrophic lifestyle [20]. Thus, direct biochemical characterization of the Rh50-type transporter
231 of *N. inopinata* would be an intriguing next step.

232 **Urea oxidation in marine environments**

233 Previous field studies have reported high urea oxidation rates in marine environments, however,
234 whether these transformations are solely attributed to a single group of organisms or involve a
235 consortium of urea-hydrolyzing microbe and AOM species remains unresolved [21]. Incubation
236 experiments in the Gulf of Mexico using urea isotope labeling suggest that marine AOA can
237 directly oxidize a significant portion of urea-N without cross-feeding interactions [22]. However, it
238 should be noted that in incubations amended with unlabeled ammonia, the rates of ^{15}N-nitrite
239 production (1.9-16.9 nM/day) were considerably lower than in those without added ^{14}N-
240 ammonia (24.5-58.7 nM/day), indicating that the presence of ammonia limited urea utilization by
241 marine AOA [22]. In addition, Tolar *et al.* measured the release of ^{15}N-ammonia in seawater
242 samples amended with ^{15}N-labeled urea to investigate the contribution of urea hydrolysis to the
243 ammonia pool [23]. They found that ~20% of the ^{15}N-label from urea was converted into ^{15}N-
244 labeld ammonia in coastal and open ocean waters, suggesting that at least ~20% of free ammonia
245 released from urea hydrolysis can fuel other ammonia oxidation or assimilation processes [23].
246 Moreover, reports of the absence of *ureC* transcription, despite the presence of *ureC* genes in
247 marine AOA natural populations, add to the complexity of the issue [24]. In summary, existing
248 gene expression and rate measurement-based field studies have not provided coherent and
249 definitive conclusions regarding direct urea oxidation by marine AOA in marine environments.
250 Additional studies are required to further explore urea oxidation activities in the open ocean and
251 mesopelagic layers. In addition to the suggested competitive advantages of utilizing both
252 ammonia and urea, we observed that *Nitrosopumilus*-like marine AOA can increase their affinity

253 for ammonia upon ammonia depletion (Fig. 3). This finding suggests an additional adaptive
254 capacity that enables marine AOA to more efficiently scavenge ammonia released from the
255 decomposition of urea or other organic matters by surrounding microorganisms.

256 **Initial description of the ureolytic capacity of *Nitrosospira lacus***

257 It was previously shown via nitrite accumulation that *Nitrosospira lacus* is uerolytic [25].
258 However, those experiments did not reveal any N substrate preference. Our comprehensive
259 monitoring of all N species and ^{15}N isotope labeling during growth revealed the unexpected
260 preferential utilization of urea over ammonia in β-AOB (Figs. 1d and 2). This finding
261 underscores the importance of nitrogen uptake regulation for nitrogen metabolism of different
262 AOM lineages. In addition, we observed in the mixed media that the specific growth rates of *N.*
263 *lacus* and *N. ureae* on urea were comparable or even higher than on ammonia (Fig. 1d and f).
264 These results provide a mechanistic basis for the initial findings reported by Urakawa *et al* [25].

265 **Potential adaptation of non-ureolytic β-AOB in the environment**

266 Our comparative genomics analysis reveals the widespread capacity for urea uptake and
267 utilization among β-AOB (Extended Data Fig. 1b). The preference for urea utilization by β-AOB
268 may serve as an adaptive strategy, potentially reducing direct competition with AOA and
269 comammox for ammonia in ammonia-limited environments. In contrast, non-ureolytic β-AOB
270 populations lacking urease genes might possess an advantage over other AOM species in
271 transitioning in and out of dormancy in response to ammonia starvation, thereby maintaining
272 microbial persistence in environments with fluctuating energy and nutrient availability [26,27].

273 **Considerations and future research on N substrate selection among different AOM lineages**

274 The AOM species characterized in our study exhibited a diverse range of adaptive strategies to
275 coordinate growth on a mixture of ammonia and urea. We acknowledge the need for a wider
276 range of ecotypes in AOM pure cultures to further investigate the diversity of N substrate

277 preferences and the regulatory systems among globally abundant ammonia oxidizers. For
278 example, it will be of interest to investigate *Nitrosopelagic*-like marine AOA species dominant in
279 the epipelagic ocean, the Water Column B (WCB) marine AOA dominant in the mesopelagic
280 ocean, *Nitrosotalea*-like soil AOA species dominant in acidic soils, *Nitrosocosmicus*-like AOA
281 species abundant in some high-ammonia environments, as well as clade B comammox species.
282 These future studies will offer a comprehensive understanding of the N substrate selection
283 regulation in AOM and provide valuable insights into the widely observed coexistence patterns
284 of different AOM lineages in various environments.

285

286 **Supplementary Figures**

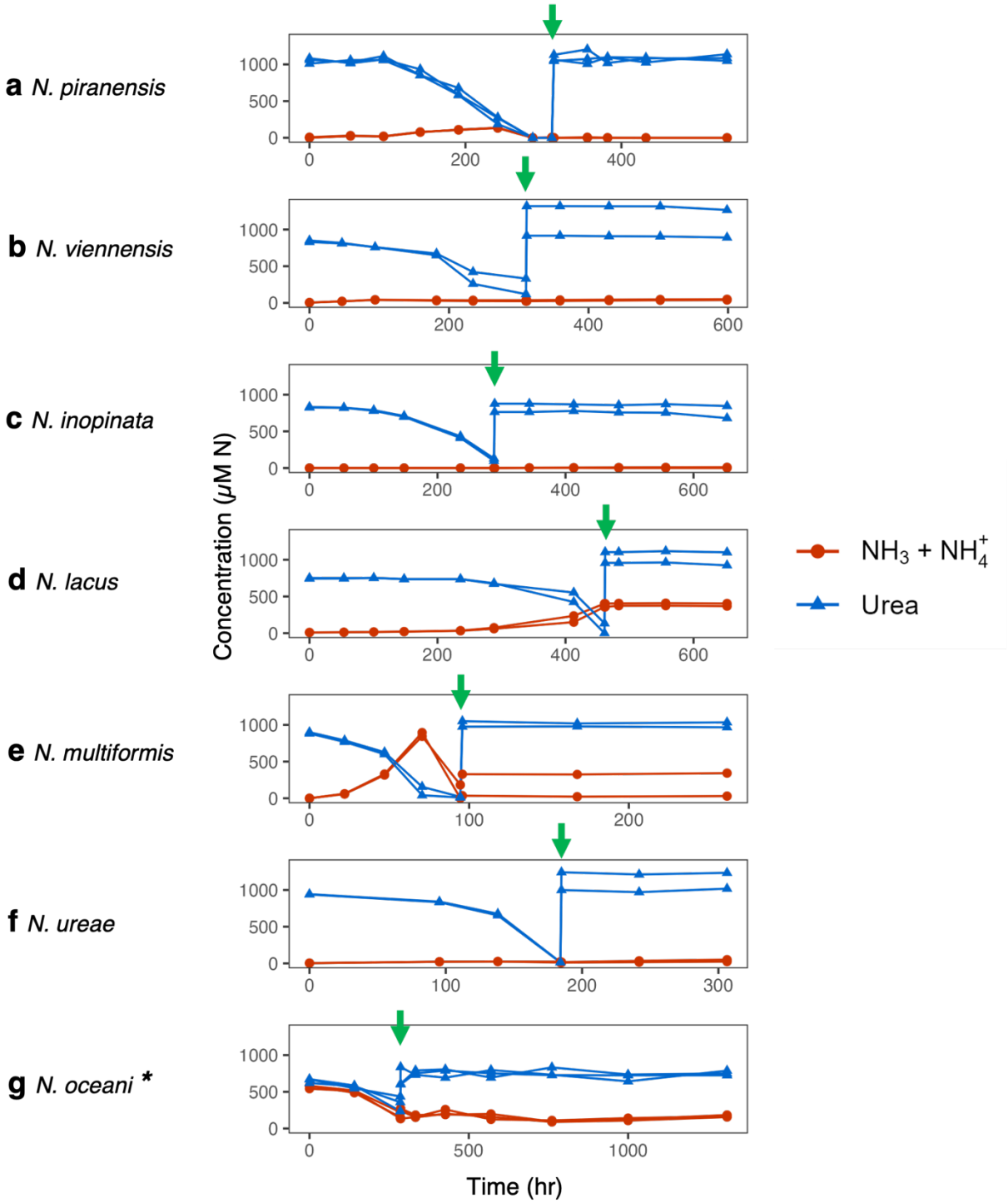

287

288 **Supplementary Figure 1. No extracellular ureolytic activity was found for marine and soil**

289 **AOA, β- and γ-AOB, and comammox species.** Concentration profiles showing the cessation of

urea utilization after removal of cells for (**a**) *N. piranensis* (marine AOA), (**b**) *N. viennensis* (soil AOA), (**c**) *N. inopinata* (comammox), (**d**) *N. lacus* (*Nitrosospira* β-AOB), (**e**) *N. multiformis* (*Nitrosospira* β-AOB), (**f**) *N. ureae* (*Nitrosomonas* β-AOB), and (**g**) *N. oceani* (γ-AOB). Lines of the same shape/color represent biological replicates. Green arrow: time of cell removal (via 0.2 μm filter) and re-addition of urea media. *Ammonia was supplied along with urea because the presence of ammonia is needed for normal rate of urea consumption by *N. oceani*. Note that neither were signal peptides identified in the urease genes of these characterized AOM species, nor were secretion system genes found in the flanking regions of the urease operons, further supporting the cytoplasmic localization of their urease enzymes.

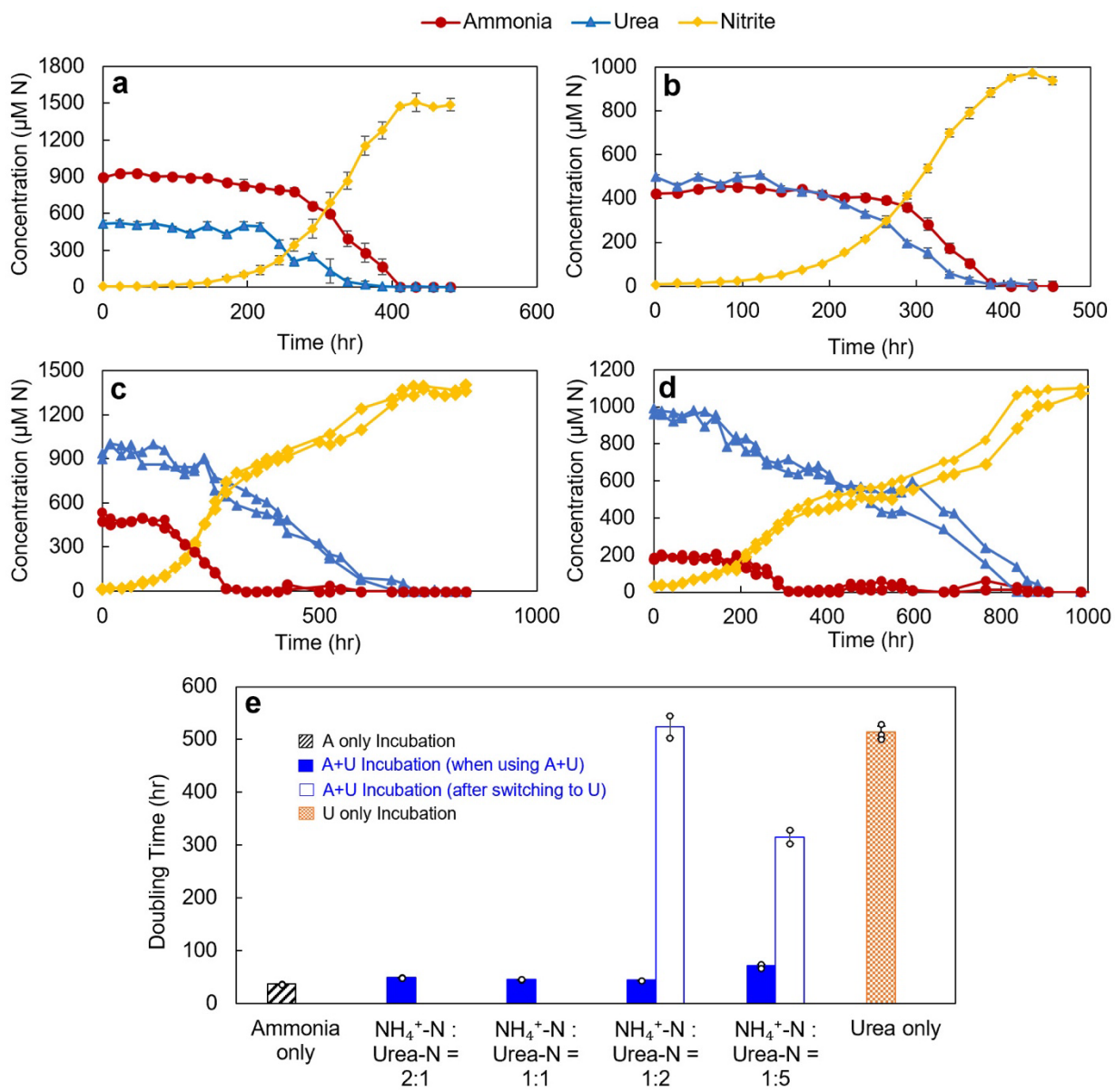

Supplementary Figure 2. Nitrogen source consumption of *Nitrosococcus oceani* grown in medium with different concentrations of ammonia and urea. Incubation with ammonia-N:urea-N ratio of (**a**) 2:1, (**b**) 1:1, (**c**) 1:2, and (**d**) 1:5. **e**, Comparison of *N. oceani* doubling time when grown in ammonia-only media, mixtures with different ammonia:urea ratios, and urea-only media. **a** and **b**, Error bars show the standard deviation of biological triplicates. **c** and **d**, Lines of the same shape/color represent biological duplicates. **e**, Note that some error bars are too

306 small to be visible, and error bars for the 1:2 and 1:5 incubations indicate the range of values

307 from biological duplicates.

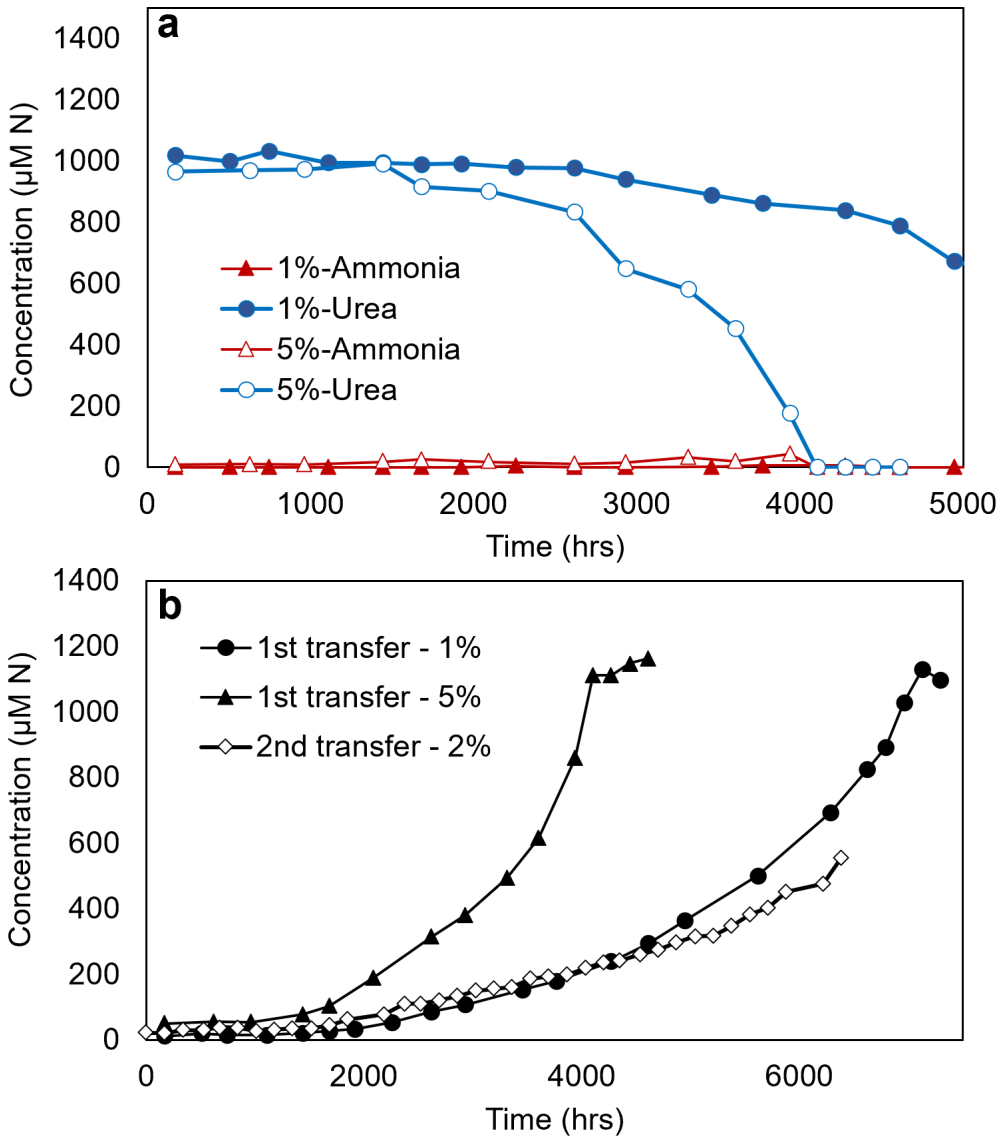

Supplementary Figure 3. Extremely slow urea consumption and nitrite production of *Nitrosococcus oceani* in urea-only medium. Due to the slow growth rate of *N. oceani* in urea-only medium, only two transfers were conducted. No appreciable increase in specific growth rate (0.03 d^{-1}) was found following the transfer of urea-grown *N. oceani* into fresh urea-only medium. **a**, Concentrations of ammonia and urea of two incubations (1% and 5% inoculum) from the 1st transfer. **b**, Nitrite accumulation growth curves of the 1st and 2nd (2% inoculum) transfers.

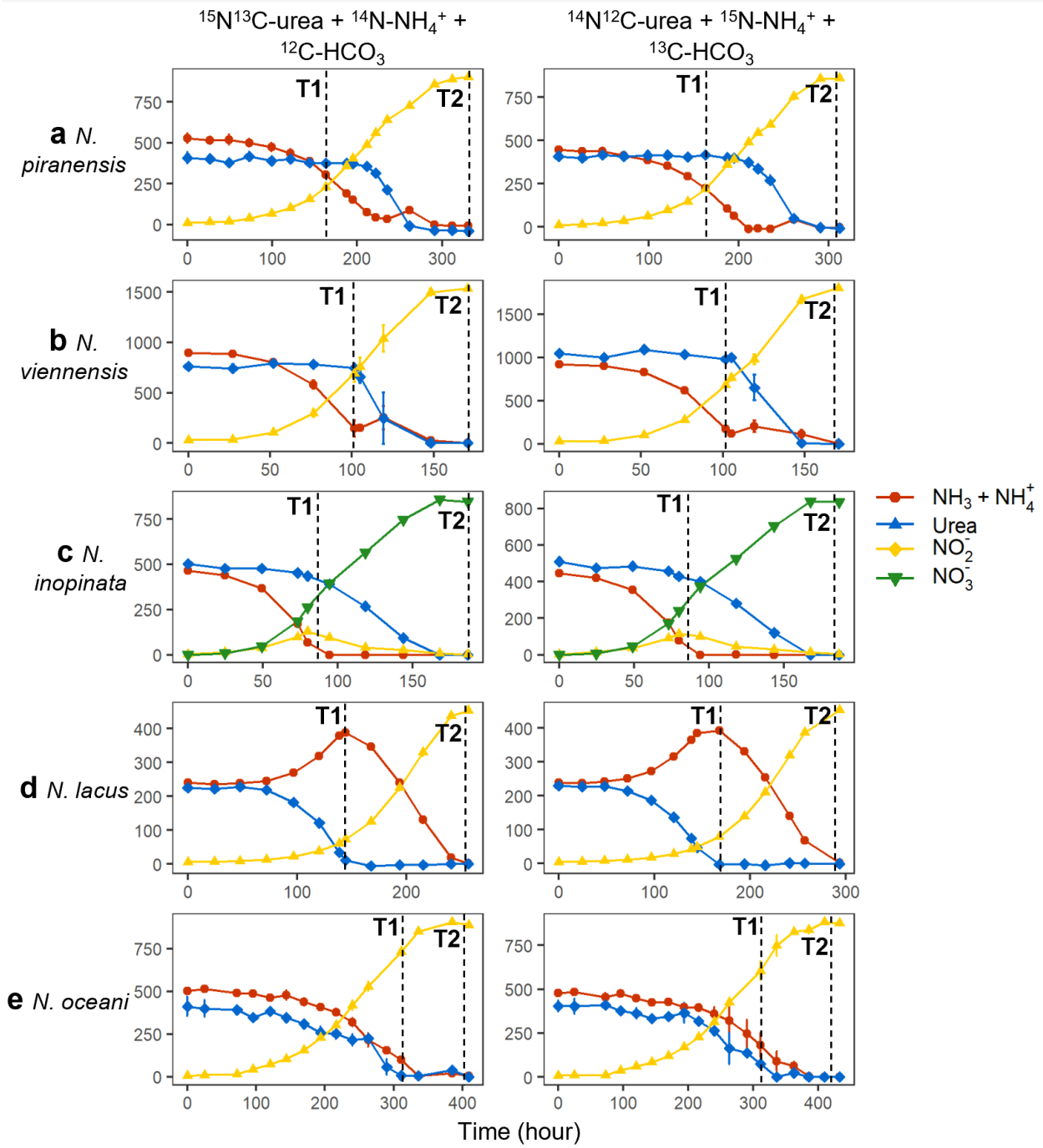

Supplementary Figure 4. Nitrogen nutrient data of incubations conducted for the NanoSIMS analysis. T1 and T2 indicate the two time points when cells were collected. (**a**) *N. piranensis* (marine AOA), (**b**) *N. viennensis* (soil AOA), (**c**) *N. inopinata* (comammox), (**d**) *N. lacus* (β-AOB), and (**e**) *N. oceani* (γ-AOB). Markers and error bars are average and one standard

321 deviation of biological triplicates except for the *N. viennensis* $^{15}N\text{-}NH_4^+$ + $^{13}C\text{-}HCO_3$ incubation

322 (b, right), where error bars indicate the maximum and minimum values of two biological

323 replicates.

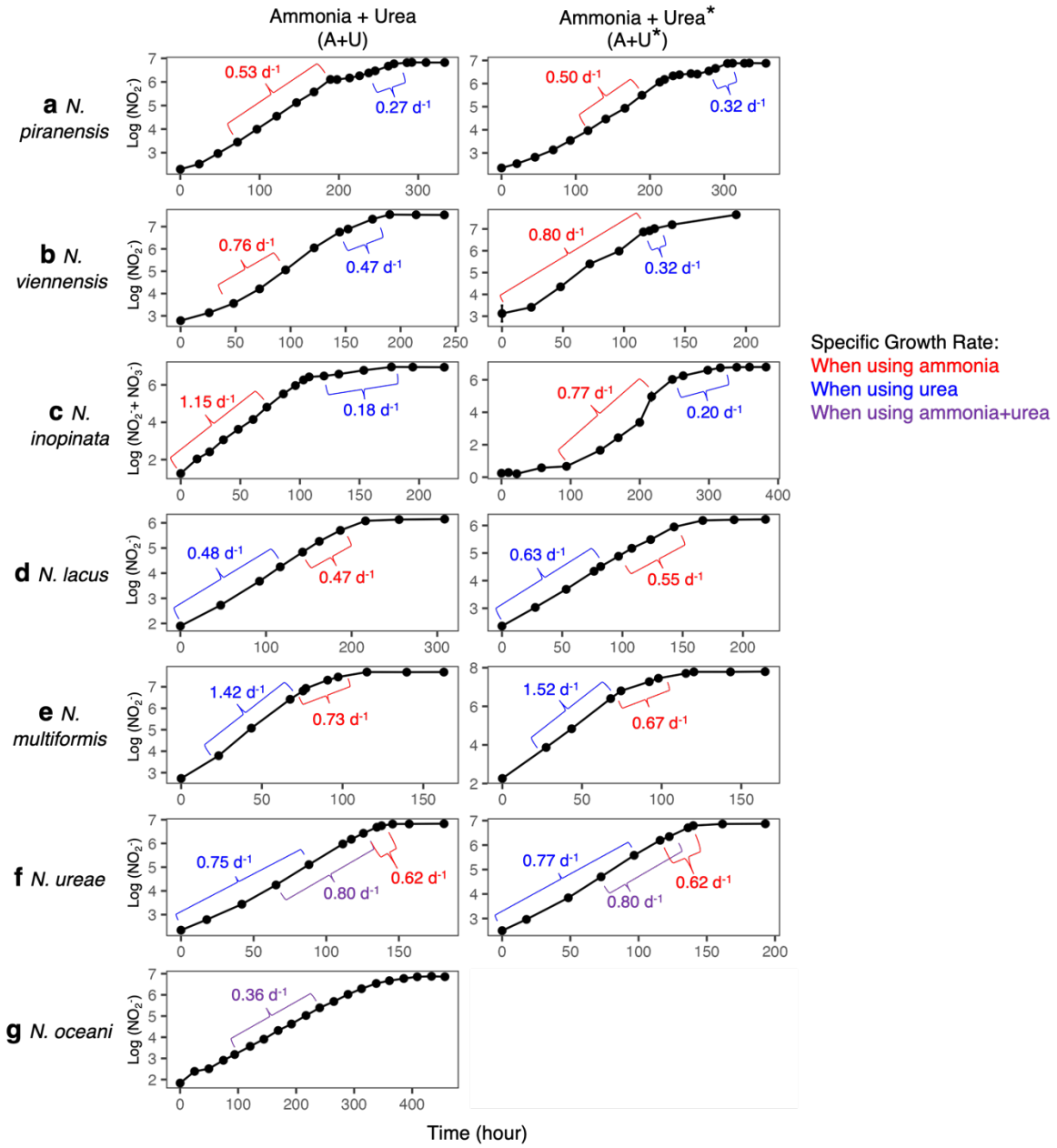

Supplementary Figure 5. Region of growth curves used to calculate the μ_{max} in Fig. 1 for the ammonia plus urea (A+U) incubations. (a) *N. piranensis* (marine AOA), (b) *N. viennensis* (soil AOA), (c) *N. inopinata* (comammox), (d) *N. lacus* (*Nitrosospira* β-AOB), (e) *N. multiformis* (*Nitrosospira* β-AOB), (f) *N. ureae* (*Nitrosomonas* β-AOB), and (g) *N. oceani* (γ-AOB). The A+U incubations were inoculated with 1% ammonia-grown culture whereas the A+U* incubations were inoculated with 1% urea-grown culture at mid-exponential phase.

Markers and error bars are average and one standard deviation of biological triplicates. The standard deviation is smaller than the marker if error bar is not visible. Urea-only incubations inoculated with urea-grown culture were not conducted for *N. oceani* due to the extremely slow growth rate.

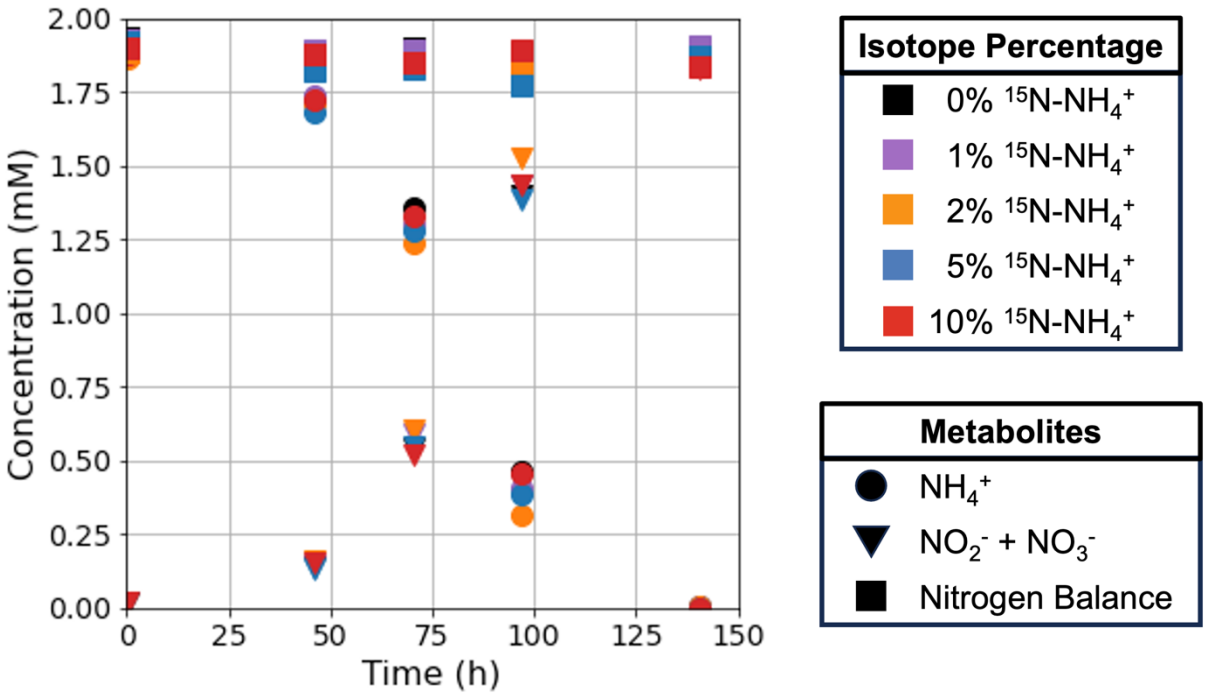

335

336 **Supplementary Figure 6. The ammonia oxidation activity of *N. inopinata* showed no**

337 **discernible effect when varying ^{15}N substrate labeling percentages from 1 to 10%.**

338

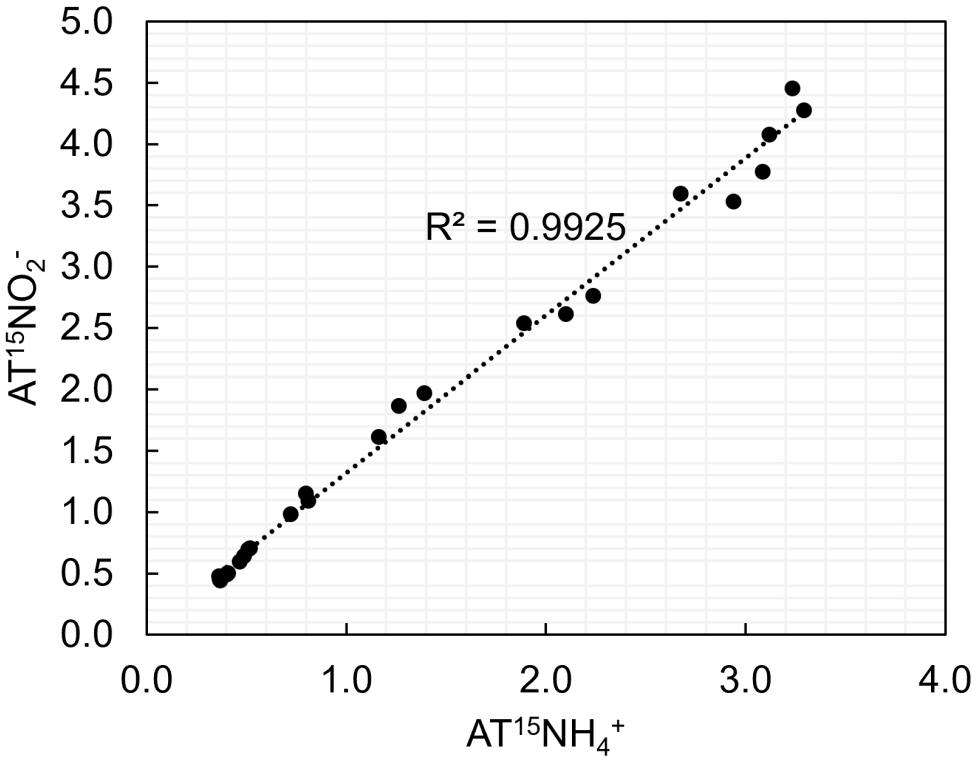

Supplementary Figure 7. Linear correlation between the newly produced ^{15}N-NO_2^- and released ^{15}N-NH_3 by *Nitrosococcus oceani* in the growth experiments supplemented with ^{15}N-urea. The linear regression line is $y = 1.284x + 0.0341$ ($R^2 = 0.9925$).

344 **Supplementary Tables**

345 Supplementary Table 1. *P*-values from two-tailed t-test ($\alpha = 0.05$) pairing the maximum specific
346 growth rate between different incubation experiments. Values less than 0.05 are highlighted in
347 green. Letters without square brackets indicate treatment with different N substrates: A =
348 incubation with ammonia only; A+U = incubation with ammonia + urea; U = incubation with
349 urea only. Letters in square brackets indicate the substrate being utilized when calculated for the
350 μ_{max}: A = when using ammonia; U = when using urea; A+U = when using ammonia and urea
351 together. *Inoculation with 1% urea-grown maintenance culture at mid-exponential phase; all
352 other incubations were inoculated with 1% ammonia-grown maintenance culture.

353

354 Supplementary Table 2. The summarized ammonia- and urea-dependent oxidation kinetics
355 parameters of *N. piranensis*, *N. viennensis*, *N. inopinata*, *N. lacus*, and *N. multiformis*.

356

357 Supplementary Table 3. The summarized transcription data of ammonia and urea uptake and
358 utilization gene in AMO species.

359

360

361

362

363

364 Supplementary Table 4. Description of the time points collected for RNA sequencing for each
365 tested AOM species.

AOM	Experi-ment	Time point 1	Time point 2	Time point 3	Time point 4
N. piranensis	AU	Exponential phase on ammonia	24 hr after urea spike	End of lag phase	Exponential phase on urea
	UA	Exponential phase on urea	24 hr after ammonia spike	Exponential phase on ammonia and urea	n/a
N. viennensis	AU	Exponential phase on ammonia	24 hr after urea spike	n/a	n/a
	UA	Exponential phase on urea	24 hr after ammonia spike	n/a	n/a
N. inopinata	AU	Exponential phase on ammonia	24 hr after urea spike	Exponential phase on urea	n/a
	UA	Exponential phase on urea	24 hr after ammonia spike	Right before ammonia depletion	n/a
N. lacus	A+U	Exponential phase on urea	8 hr before urea depletion	Exponential phase on ammonia	n/a
N. oceani	AU	Exponential phase on ammonia	24 hr after urea spike	Exponential phase on ammonia and urea	n/a
	UA	Not conducted due to extremely slow specific growth rate in urea-only medium.			

366

367

368 **Source data**

369 Source Data Table 1. Differential transcription of all AMO species genes in response to
370 ammonia and urea additions.

371 Source Data Table 2. NanoSIMS analysis output ("Raw") and processed data ("Data") for
372 calculating substrate incorporation percentages.

373

374 **References**

375 1 Koch, H. *et al.* Expanded metabolic versatility of ubiquitous nitrite-oxidizing bacteria from the
376 genus *Nitrospira*. *Proc. Natl. Acad. Sci. U.S.A.* **112**, 11371-11376 (2015).
377 2 Li, J. *et al.* Selective enrichment and metagenomic analysis of three novel comammox *Nitrospira*
378 in a urine-fed membrane bioreactor. *ISME commun.* **1**, 7 (2021).
379 3 Huergo, L. F., Chandra, G. & Merrick, M. P_{II} signal transduction proteins: nitrogen regulation and
380 beyond. *FEMS Microbiol. Rev.* **37**, 251-283 (2013).
381 4 Leigh, J. A. & Dodsworth, J. A. Nitrogen regulation in bacteria and archaea. *Annu. Rev. Microbiol.*
382 **61**, 349-377 (2007).
383 5 Forchhammer, K., Selim, K. A. & Huergo, L. F. New views on P_{II} signaling: from nitrogen sensing
384 to global metabolic control. *Trends Microbiol.* (2022).
385 6 Emori, M. T. *et al.* The deuridylylation activity of Herbaspirillum seropedicae GlnD protein is
386 regulated by the glutamine: 2-oxoglutarate ratio. *Biochim. Biophys. Acta Proteins Proteom. BBA-*
387 *PROTEINS PROTEOM* **1866**, 1216-1223 (2018).
388 7 Merrick, M. Post-translational modification of P_{II} signal transduction proteins. *Front. Microbiol.*
389 **5**, 763 (2015).
390 8 Qin, W. *et al.* Stress response of a marine ammonia-oxidizing archaeon informs physiological
391 status of environmental populations. *ISME J* **12**, 508-519 (2018).
392 9 Offre, P., Kerou, M., Spang, A. & Schleper, C. Variability of the transporter gene complement in
393 ammonia-oxidizing archaea. *Trends Microbiol.* **22**, 665-675 (2014).
394 10 Nakagawa, T. & Stahl, D. A. Transcriptional response of the archaeal ammonia oxidizer
395 *Nitrosopumilus maritimus* to low and environmentally relevant ammonia concentrations. *Appl.*
396 *Environ. Microbiol.* **79**, 6911-6916 (2013).
397 11 Watzer, B. *et al.* The signal transduction protein P_{II} controls ammonium, nitrate and urea uptake
398 in Cyanobacteria. *Front. Microbiol.* **10** (2019).
399 12 Ernst, F. D. *et al.* The nickel-responsive regulator NikR controls activation and repression of gene
400 transcription in Helicobacter pylori. *Infect. Immun.* **73**, 7252-7258 (2005).
401 13 Jung, M.-Y. *et al.* Ammonia-oxidizing archaea possess a wide range of cellular ammonia
402 affinities. *ISME J* **16**, 272-283 (2022).
403 14 Button, D. K. Nutrient uptake by microorganisms according to kinetic parameters from theory as
404 related to cytoarchitecture. *Microbiol. Mol. Biol. Rev.* **62**, 636-645 (1998).
405 15 Cherif-Zahar, B. *et al.* Evolution and functional characterization of the *RH50* Gene from the
406 ammonia-oxidizing bacterium *Nitrosomonas europaea*. *J. Bacteriol.* **189**, 9090-9100 (2007).
407 16 Kim, M. *et al.* Need-based activation of ammonium uptake in *Escherichia coli*. *Mol. Syst. Biol.* **8**,
408 616 (2012).
409 17 Weidinger, K. *et al.* Functional and physiological evidence for a Rhesus-type ammonia
410 transporter in *Nitrosomonas europaea*. *FEMS Microbiol. Lett.* **273**, 260-267 (2007).
411 18 Lupo, D. *et al.* The 1.3-A resolution structure of *Nitrosomonas europaea* Rh50 and mechanistic
412 implications for NH_3 transport by Rhesus family proteins. *Proc. Natl. Acad. Sci. U.S.A.* **104**,
413 19303-19308 (2007).
414 19 Ganz, P. *et al.* A twin histidine motif is the core structure for high-affinity substrate selection in
415 plant ammonium transporters. *J. Biol. Chem.* **295**, 3362-3370 (2020).
416 20 Kits, K. D. *et al.* Kinetic analysis of a complete nitrifier reveals an oligotrophic lifestyle. *Nature*
417 **549**, 269-272 (2017).
418 21 Laperriere, S. M. *et al.* Nitrification and nitrous oxide dynamics in the Southern California Bight.
419 *Limnol. Oceanogr.* **66**, 1099-1112 (2021).

420 22 Kitzinger, K. *et al.* Cyanate and urea are substrates for nitrification by Thaumarchaeota in the
421 marine environment. *Nat. Microbiol.* **4**, 234-243 (2019).
422 23 Tolar, B. B., Wallsgrove, N. J., Popp, B. N. & Hollibaugh, J. T. Oxidation of urea-derived nitrogen
423 by thaumarchaeota-dominated marine nitrifying communities. *Environ. Microbiol.* **19**, 4838-
424 4850 (2017).
425 24 Smith, J. M., Damashek, J., Chavez, F. P. & Francis, C. A. Factors influencing nitrification rates and
426 the abundance and transcriptional activity of ammonia-oxidizing microorganisms in the dark
427 northeast Pacific Ocean. *Limnol. Oceanogr.* **61**, 596-609 (2016).
428 25 Urakawa, H. *et al. Nitrosospira lacus* sp. nov., a psychrotolerant, ammonia-oxidizing bacterium
429 from sandy lake sediment. *Int. J. Syst. Evol. Microbiol.* **65**, 242-250 (2015).
430 26 Berube, P. M., Samudrala, R. & Stahl, D. A. Transcription of all *amoC* copies is associated with
431 recovery of *Nitrosomonas europaea* from ammonia starvation. *J. Bacteriol.* **189**, 3935-3944
432 (2007).
433 27 French, E. & Bollmann, A. Freshwater ammonia-oxidizing archaea retain *amoA* mRNA and 16S
434 rRNA during ammonia starvation. *Life* **5**, 1396-1404 (2015).

435